Ann. Geophys., 27, 933–942, 2009
www.ann-geophys.net/27/933/2009/

Annales Geophysicae

Naturally enhanced ion-line spectra around the equatorial 150-km region

J. L. Chau[1], **R. F. Woodman**[1], **M. A. Milla**[2], **and E. Kudeki**[2]

[1]Radio Observatorio de Jicamarca, Instituto Geofísico del Perú, Lima
[2]Electrical and Computer Engineering, University of Illinois at Urbana-Champaing, IL, USA

Received: 31 October 2008 – Revised: 28 January 2009 – Accepted: 30 January 2009 – Published: 2 March 2009

Abstract. For many years strong radar echoes coming from 140–170 km altitudes at low latitudes have been associated to the existence of field-aligned irregularities (FAIs) (the so called 150-km echoes). In this work, we present frequency spectra as well as angular distribution of 150-km echoes. When the 150-km region is observed with beams perpendicular to the magnetic field (**B**) the observed radar spectra are very narrow with spectral widths between 3–12 m/s. On the other hand, when few-degrees off-perpendicular beams are used, the radar spectra are wide with spectral widths comparable to those expected from ion-acoustic waves at these altitudes (>1000 m/s). Moreover the off-perpendicular spectral width increases with increasing altitude. The strength of the received echoes is one to two orders of magnitude stronger than the expected level of waves in thermal equilibrium at these altitudes. Such enhancement is not due to an increase in electron density. Except for the enhancement in power, the spectra characteristics of off-perpendicular and perpendicular echoes are in reasonable agreement with expected incoherent scatter spectra at these angles and altitudes. 150-km echoes are usually observed in narrow layers (2 to 5). Bistatic common volume observations as well as observations made few kilometers apart show that, for most of the layers, there is very high correlation on power fluctuations without a noticeable time separation between simultaneous echoes observed with Off-perpendicular and Perpendicular beams. However, in one of the central layers, the echoes are the strongest in the perpendicular beam and absent or very weak in the off-perpendicular beams, suggesting that they are generated by a plasma instability. Our results indicate that most echoes around 150-km region are not as aspect sensitive as originally thought, and they come from waves that have been enhanced above waves in thermal equilibrium.

Correspondence to: J. L. Chau
(jchau@jro.igp.gob.pe)

Keywords. Ionosphere (Equatorial ionosphere; Ionospheric irregularities; Instruments and techniques)

1 Introduction

Relatively strong suprathermal signals from the upper E region (140–170 km) equatorial ionosphere are observed routinely during daytime hours over the Jicamarca Radio Observatory. Such echoes, called 150-km echoes, were first reported by Balsley (1964) and later associated to field-aligned irregularities (FAIs) by Røyrvik and Miller (1981) and Røyrvik (1982). Very little attention was given to these echoes until the very high-resolution observations were reported by Kudeki and Fawcett (1993). Besides the new characteristics of the echoes, Kudeki and Fawcett (1993) suggested the possible use of their radial velocities to measure the equatorial F region **E**×**B** drifts using low power systems. The technique was later validated against simultaneous Incoherent Scatter Radar (ISR) drifts (Woodman and Villanueva, 1995), since then, 150-km echoes are being used to monitor the equatorial daytime electric fields on routine basis (e.g. Chau and Woodman, 2004; Anderson et al., 2004). Although drifts from 150-km echoes are being used to diagnose the equatorial ionosphere, their generation mechanism remains unknown.

Until recently 150-km echoes were thought to be confined to the equatorial electrojet (EEJ) region since they were observed at other equatorial sites with similar temporal, altitude and spectral characteristics to those observed over Jicamarca (e.g. Blanc et al., 1996; Kudeki et al., 1998; de Paula and Hysell, 2004; Tsunoda and Ecklund, 2004). Nowadays we know that similar echoes are also observed at latitudes outside the EEJ belt (India, Indonesia) at comparable altitudes (e.g. Choudhary et al., 2004; Patra and Rao, 2006; Patra et al., 2008). All of these observations have been made with beams pointing perpendicular to the magnetic field (**B**), and

Published by Copernicus Publications on behalf of the European Geosciences Union.

Table 1. Parameters for perpendicular and off-perpendicular 150-km experiments at Jicamarca.

Parameter	Two-beam	Bistatic
Date	Dec 2004	Mar 2008
Effective IPP (km)	110	187.5
Nyquist (m/s)	2040	1200
FFT points	32	8000
Resolution (km)	0.75	0.75
Transmitter power (MW)	2	2
Rx Perp. Antenna	150 m×150 m	32 m×16 m
Mode	Interleaved	Simultaneous
Code	Barker 7	Barker 13

therefore the echoes have been associated to FAIs. Moreover, aspect sensitivity measurements using interferometry have reported values between the EEJ and equatorial spread F (ESF) aspect angles with values less than 0.1° (e.g. Fawcett, 1999; Lu et al., 2008).

Since 150-km echoes have been associated to FAIs, current hypothesis have tried to find the free-energy source that could generate the plasma irregularities (e.g., Kudeki and Fawcett, 1993; Patra and Rao, 2006; Tsunoda and Ecklund, 2004). So far none of the hypothesis are able to explain the generation mechanism and to reproduce all the observations. Moreover, 150-km echo features appear to be dependent on longitude sector. For example, the signal strength of 150-km echoes present a strong summer dependance over Pohnpei (Tsunoda and Ecklund, 2004) while there is very little seasonal dependence over Jicamarca (Chau and Kudeki, 2006a) and Gadanki (Patra and Rao, 2007).

A surprising observation was reported by Chau (2004). He reported enhanced echoes around 150-km region but using a beam pointing 1.83° off-perpendicular to **B**. The echoes were strong and presented similar time and altitude dependence to the usual 150-km echoes coming from exact perpendicular conditions, i.e., necklace shape with early morning descent and afternoon ascent, temporal modulation of the echo intensity with periods between 5 to 10 min and organized in 2–4 thin layers (e.g. Kudeki and Fawcett, 1993). Moreover the spectra were very wide, much wider than typical 150-km Perpendicular spectra, with widths corresponding to velocities larger than 1000 m/s. Similar spectra characteristics are expected from ISR spectra at these altitudes, but not with the observed enhanced power (more than 10 dB). At first, we thought that the echoes were coming from enhanced density layers. Recall that in IS theory the power is proportional to the electron density. In fact, to check this possibility we carried out a Faraday rotation experiment, a method for determining the absolute electron density profile that is independent of the scattering mechanism (e.g. Farley, 1969). The results were negative (Woodman and Chau, 2005). In addition, the lack of a reflecting layer at these altitudes in corresponding ionograms, excludes this possibility.

In order to help the presentation and discussion of the results below, it is important to recall that IS spectra obtained from angles close to perpendicular to **B** present unique shapes. At small angles around perpendicularity, the IS spectra shape go from very narrow, controlled by the dynamics of the gyrating electrons bound to the magnetic field lines, to wide, controlled by the velocity of free streaming ions. The transition occurs at a critical angle of ∼0.334°, where the projection of the electron gyro-center thermal velocities along the line of sight of the radar is comparable to the ion velocity (e.g. Woodman, 2004). For angles slightly larger than the critical angle, the IS spectra start to present similar shapes to so-called IS ion-line spectra observed at other ISRs, i.e., wide spectra with two humps.

In this work, we present simultaneous measurements of perpendicular and off-perpendicular (Off-Perp) 150-km echoes using a two-beam and bistatic configurations. With the two beams, the observed volumes are separated ∼5 km in the meridional direction, while using the bistatic system both echoes come from the same volume. In addition, to the range and altitude characteristics of the observed echoes, we present the spectra shape of the off-perpendicular echoes as well as the temporal and altitude characteristics of approximate spectral widths. Comparing the power measured with the two-beam configuration, we present and discuss the new aspect sensitivity results, this time using all frequency components of the spectra. Finally, we discuss our results based on the two type of 150-km echoes observed.

2 Experiments setup

We have used the Jicamarca incoherent scatter radar and a second receiving antenna to observe both perpendicular and the off-perpendicular 150-km echoes at 50 MHz. Such observations have been made using two configurations which we call (1) the two-beam and (2) the bistatic, configurations. A sketch of both configurations is shown in Fig. 1.

For the two-beam configuration, we used one polarization of the 300 m×300 m Jicamarca antenna to transmit and receive pointing perpendicular, and the other polarization to get the off-perpendicular (1.83°) observations. For both beams, a two-antenna interferometer, aligned in the north-south direction, using quarter sections was used on reception, employing the same polarization used for transmission. To avoid aliasing of the frequency spectrum a short interpulse period (IPP) of 110 km (or ∼0.73 ms) was used. This configuration causes range aliasing of F region ISR echoes on the expected 150-km range gates, but with much lower amplitudes than the enhanced 150-km echoes. Furthermore, to avoid cross-talk between beams, each beam was interleaved every 34 IPPs (∼25 ms). The observed volumes of the two beams were separated ∼5 km in the North-South direction. For each beam, 2 MW peak power was used with a coded pulse allowing an effective range resolution of 0.75 km (see Table 1). The back scatter radar aperture (ABS) difference between the two antenna beams was ∼3.9 dB (Off-Perpendicular minus Perpendicular). Such experiment was conducted on 10 December 2004.

The bistatic experiment was conducted on 3 April 2008. Again one of the main Jicamarca polarizations was used for transmission and reception pointing at the off-perpendicular direction (1.83°), while a small antenna array consisting of 8×4 4-element Yagi antennas (∼32 m×16 m) was used to receive echoes from the same illuminated volume. The small array was located ∼10 km south of Jicamarca, allowing the bistatic Bragg scattering vector to point perpendicular to **B** around the 150-km region. For all practical purposes, for the bistatic configuration, both echoes, perpendicular and off-perpendicular, came from the same volume. To avoid the contamination of mountain clutter and improve the frequency resolution of the spectra measurements, this time we used an IPP of 187.5 km. The resulting spectra are frequency aliased at the upper altitudes, but the measurements are good enough to get qualitative characteristics of the off-perpendicular signal. The acquisition systems of both sites were synchronized using the 1 pulse per second (PPS) from GPS receivers, allowing a time synchronization with an accuracy of <30 ns. The master oscillators of both systems were GPS disciplined to synchronize them in frequency.

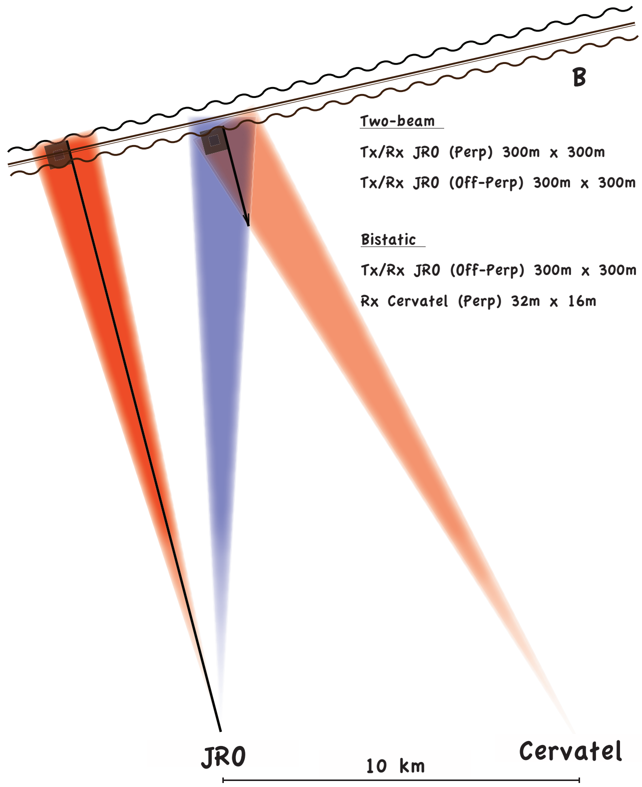

Fig. 1. Experiment configuration. **(a)** The two-beam configuration uses two independent beams from Jicamarca to point perpendicular (dark red) and off-perpendicular (blue), respectively. **(b)** The bistatic configuration uses one Jicamarca beam to point off-perpendicular (blue) and simultaneously a beam from Cervatel (ligh red) is used for reception. The combined Cervatel-Jicamarca link points perpendicular to **B** at 150-km altitude. The separation between sites is ∼10 km.

3 Results

As mentioned above, we have conducted two types of experiments to observe perpendicular and off-perpendicular 150-km echoes.

3.1 Two-beam results

In Fig. 2 we show altitude-time signal-to-noise (SNR) contour plots for three signals obtained from the two-beam experiment. In the top row we show the SNR contour plot of the low-frequency component of the perpendicular data. To get insight the low frequency information, we have coherently integrated the data for ∼0.05 ms. A similar procedure is typically used at other sites, given that 150-km echoes when observed with perpendicular echoes present very narrow spectral width (<20 m/s). In the middle row we show the SNR contour plot of the perpendicular data, but this time using the information of all the frequency components. To compare the signal intensities of the echoes between off-perpendicular and perpendicular beams, we have compensated the SNR values of the perpendicular beam by the ABS ratio (i.e., we have added 3.9 dB). Both contour plots show essentially the same information, namely (a) four layers, (b) temporal modulations with periods between 5–10 min, (c) the third layer (from top to bottom) is wider than the other layers, and (d) the strongest echoes come from the third layer.

The bottom row in Fig. 2 shows the SNR contour plot for the off-perpendicular data using all the frequency bins after using a 3-point median filter. This filter removes possible perpendicular echoes coming via antenna sidelobes. The off-perpendicular SNR plot shows (a) four layers, (b) temporal modulation with periods between 5–10 min, (c) the third layer is narrower than the upper two layers, and (d) the strongest echoes come from the upper two layers.

Comparing the perpendicular and off-perpendicular SNR results, we find that:

1. There is an excellent correlation of signal fluctuations between perpendicular and off-perpendicular echoes of layers 1, 2 and 4. Using 25 s resolution, we were not able to find a time difference between the occurrence of both echoes, even though they are separated ∼5 km in the North-South direction.

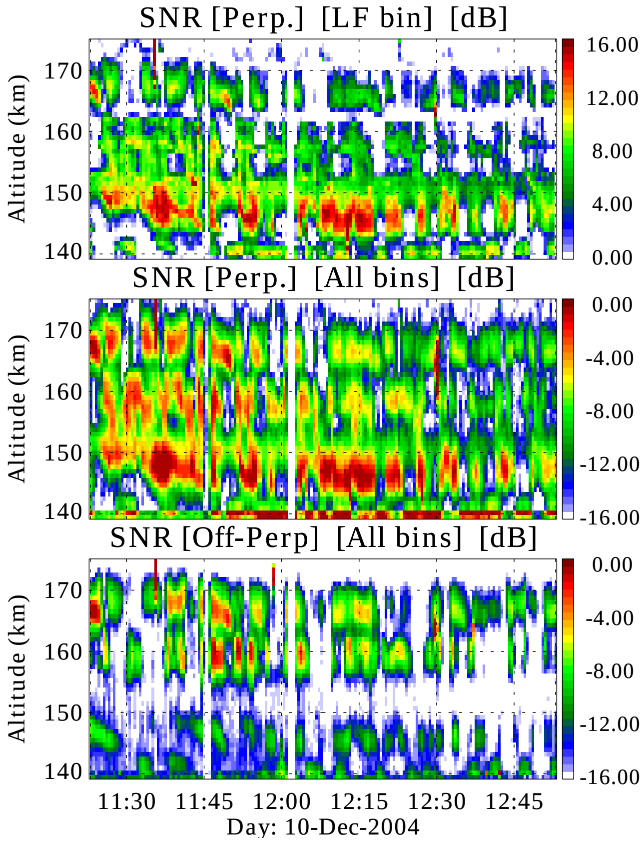

Fig. 2. Signal-to-noise ratio (SNR) contour plots for the two beam experiment conducted on 10 December 2004. **(a)** The low frequency (LF) component of the perpendicular beam after coherent integration, **(b)** using all the frequency bins for the perpendicular signal, and **(c)** the off-perpendicular signal using all frequency bins. The values are color coded with the color bar at the right of each plot.

2. The perpendicular echoes are stronger in the third layer, whereas the corresponding off-perpendicular echoes are either weaker or absent showing a poor correlation with the perpendicular echoes.

3. The perpendicular echoes on layers 1 and 2 present comparable strength to their corresponding off-perpendicular echoes.

To get more insight on the reliability of the results and the peculiarities of the analyzed data, Fig. 3 shows sample spectrograms from the data used in Fig. 2, taken between 12:15 and 12:18 LT. The top row show the low-frequency spectra components for the perpendicular data after coherent integration. Each spectrogram has been obtained after ∼1 min averaging. The middle row shows the spectrograms for the perpendicular data but for all frequency bins. Note the changes in the radial velocity axis and the SNR color coded values. Finally, the bottom row shows the spectrograms for the off-perpendicular data. Again, we have used a 3-point median filter to avoid any possible perpendicular contamination coming from antenna sidelobes. The blue background in the off-perpendicular data are due to remnants of the range aliased F region spectra that have not been completely removed.

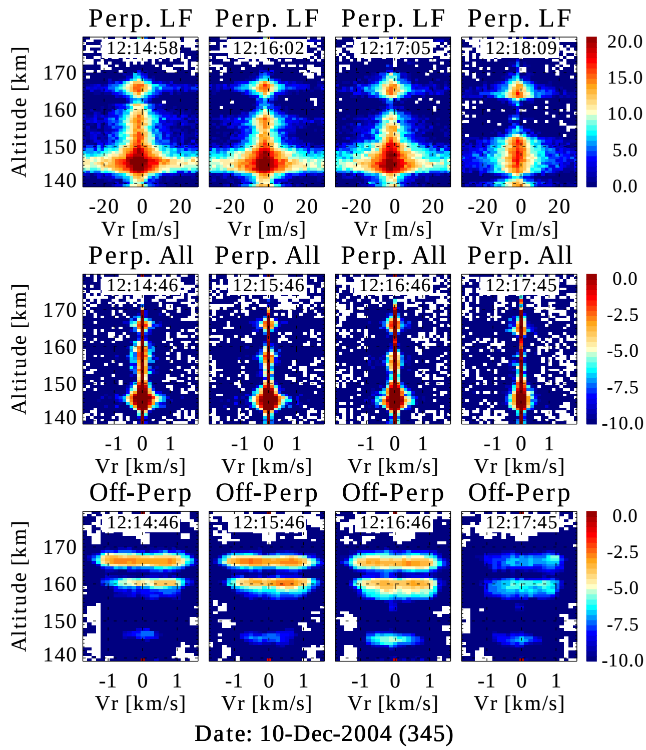

Fig. 3. Sample spectrograms for the signals used in Fig. 2 for four consecutive minutes. Each spectrogram has been averaged for 1 min. To display the spectrogram of the off-perpendicular signal, we have used a 3-point median filter. The color code for the signal intensity is displayed to the right of each row.

The salient features of Fig. 3 are:

1. The spectral widths of the low frequency spectra are less than 15 m/s as reported in previous low power perpendicular observations.

2. The low-frequency perpendicular echoes present wider spectra in the third layer. Such apparent widening is due to the signal leakage caused by the convolution with the rectangular window (middle row).

3. The perpendicular spectrograms showing all frequency bins show significant signal outside the "low frequency" (LF) bin. As in the case of typical ISR radar spectra over Jicamarca, such signature is expected for the enhanced 150-km echoes given that a finite beam is used and not all the angles are pointing perpendicular, i.e., there are other angles being observed (e.g. Woodman, 2004; Milla and Kudeki, 2006).

4. The spectra of the off-perpendicular data are very wide. The width increases with increasing altitude.

As mentioned in the Introduction, the off-perpendicular observations reported by Chau (2004) were surprising since for many years the 150-km echoes were associated to FAIs. Moreover, very small aspect angles were obtained using interferometry. Those angles were between the EEJ and ESF measured aspect angles (≤0.1°) (Fawcett, 1999; Lu et al., 2008).

In Fig. 4 we show the power ratio (Off-perpendicular/Perpendicular) using the low-frequency bins (top row) and all frequencies (bottom row) for the four time periods used in Fig. 3. The ratios have been corrected by the ABS difference of 3.9 dB. The data for each time interval are indicated with different symbols and colors. The vertical dashed line indicates the value of 1. For those times and altitudes where only signal in the perpendicular beam is present, we have assigned them an arbitrary value of 0.001 just to differentiate them from those intervals when there are not data.

Using only the low frequency bin information we see smaller power ratio values than when all the frequency bins are used, indicating that the echoes are more aspect sensitive at low frequencies, similar to IS. In general, using all the frequency bins, the power ratio increases with increasing altitude, approaching a value around 1 at the upper altitudes indicating that echoes are less aspect sensitive and close to isotropic at higher altitudes.

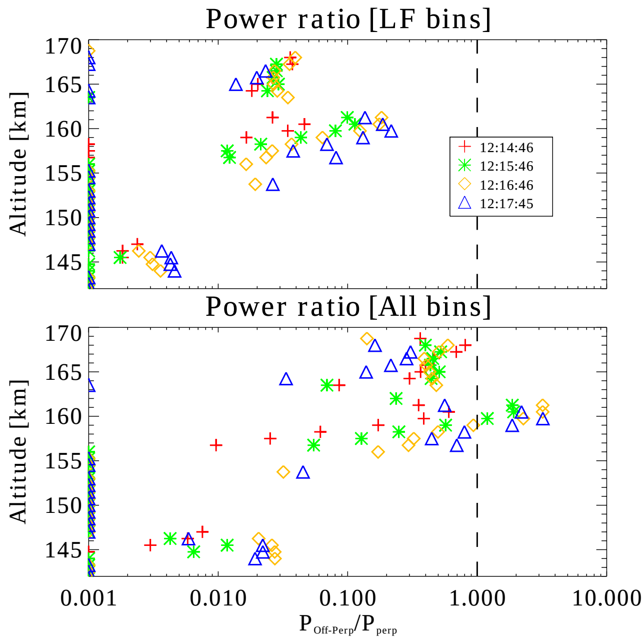

Fig. 4. Power ratio values using the off-perpendicular and perpendicular signals after correcting for the radar backscatter aperture difference. Small values indicate large aspect sensitivity. Values close to 1 indicate isotropic scattering. The top/bottom row shows the results of the low/all frequency ("LF"/"All") data. Different times are indicated with different colors. Note that when there is only power in the perpendicular beam, we are using a number of 0.001.

3.2 Bistatic results

Now we present the results of the bistatic configuration. Given that both data, off-perpendicular and perpendicular, were taken simultaneously, we have used 8000 points to calculate the spectra, allowing us to have a better identification of the low frequency components. Namely, this time we are not using coherent integrations to avoid frequency aliasing when the low frequency components are analyzed. In this case the low frequency components are composed of radial velocity bins that are within ±50 m/s. On the other hand, for getting the off-perpendicular parameters, we are not using the low frequency components to avoid possible contributions of perpendicular echoes coming from sidelobes.

In Fig. 5 we show altitude-time contour plots for the perpendicular ((a) SNR and (b) spectral width) and for the off-perpendicular ((c) SNR and (d) spectral width) data. Note that the each plot has its corresponding color bar. The spectra of the off-perpendicular data are slightly frequency aliased due to the longer IPP used than the one used in the two-beam experiment, but we think the spectra are good enough resolved as to get a qualitative idea of the their actual width.

The most important results of Fig. 5 are:

1. The echoes are again organized mainly in four layers, and present time modulations in power with periods between 5 and 10 min.

2. There is a strong correlation between off-perpendicular and perpendicular echoes occurring in layers 1, 2 and 4 (from up to down).

3. As in the case of the two beam data, the third layer present the strongest echoes on perpendicular but very weak or no echoes in the off-perpendicular data.

4. The strongest perpendicular echoes are characterized by a very narrow spectral width (see green section in Fig. 5b). This result is consistent with the Pohnpei observations (Tsunoda and Ecklund, 2000), indicating that turbulence is very weak at this layer compared to the other layers.

5. The spectral width of the off-perpendicular data shows clear altitudinal dependence, increases as altitude increases. Moreover, the off-perpendicular spectral width is independent of the power modulation observed in Fig. 5.

With the bistatic configuration, we are able to detect only Perpendicular echoes. Off-perpendicular echoes, including those close to perpendicular, are not observed given that the receiving antenna used is smaller than the one used in the two-beam data (see Table 1).

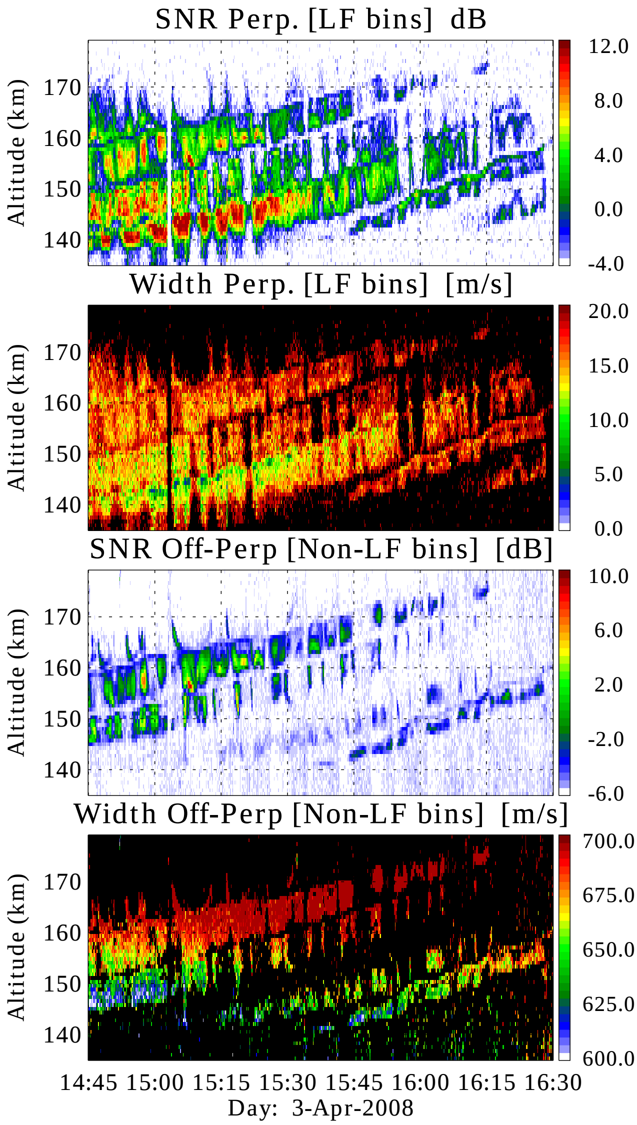

Fig. 5. Bistatic altitude-time contour maps for **(a)** perpendicular SNR, **(b)** perpendicular spectral width, **(c)** off-perpendicular SNR, and **(d)** off-perpendicular spectral width for data taken on 3 April 2008. For the perpendicular plots, only low-frequency bins are used, while for the off-perpendicular plots the low-frequency bins are not used.

4 Discussion

When Chau (2004) first reported the off-perpendicular 150-km echoes, we expected to find the missing clue for solving what some colleagues called the 150-km riddle. However, the off-perpendicular observations bring more complications to finding a single generation mechanism for both perpendicular and off-perpendicular echoes. Definitely most of the perpendicular echoes observed at Jicamarca are related to the off-perpendicular echoes and therefore to their origin. But there is clearly a layer (the third layer in the examples above) that is uniquely distinct.

Before we start the discussion of the results of this paper, we first summarize the important peculiarities of the region where these echoes occur, i.e., equatorial 140–170 km daytime ionosphere, most of them obtained from Schunk and Nagy (2000):

1. In this region occurs the transition between the dominant molecular ions of lower altitudes [NO^+, O_2^+, N_2^+] and F-region dominant atomic oxygen ion [O^+].

2. Collisions with neutrals start to be less important as the altitude increases.

3. Electron Coulomb collisions need to be consider for angles close to perpendicular, i.e., for $<3°$ (e.g. Sulzer and Gonzalez, 1999; Milla and Kudeki, 2006).

4. At the magnetic equator, magnetic field lines around 140–170 km are mapped to both the north and south E regions that are located outside the EEJ belt.

5. Intermediate layers are known to occur at these altitudes but so far they have not been observed at equatorial regions during the day.

6. Large electron to ion (and therefore neutral) temperature ratios are expected and observed during the day.

7. Maximum photoelectron production rate occurs around 150 km (e.g. Su et al., 1998).

8. Altitudes below 200 km are difficult to explore with ISR techniques due to the presence of 150-km echoes, subject of this study, and other ionospheric irregularities causing strong coherent echoes, like, EEJ, meteor head and trails (e.g. Chau and Woodman, 2005; Chau and Kudeki, 2006b).

9. Only a hand full of in-situ measurements have been performed with rockets but the probes did not observe any strong evidence for plasma irregularities (e.g. Prakash et al., 1969).

Besides these characteristics, there are other features that have been invoked in the past that could also be important, but either they have not been observed or there are very few observations. For example, there is very little information about the neutral dynamics of this region (zonal and neutral winds, tides, gravity wave activity, wind shears, etc.).

We first start with the discussion of the aspect sensitivity of 150-km echoes. As mentioned above, for many years it has been thought that 150-km echoes were produced by FAIs. Moreover, using interferometry aspect angles less than 0.1° were reported (Fawcett, 1999; Lu et al., 2008). From our results, we know now that most 150-km echoes observed over Jicamarca are not as aspect sensitive, since they can be observed at off-perpendicular angles. Besides the off-perpendicular results at 1.83°, we have also observed the upper layer echoes as far as 5° (the maximum off-perpendicular

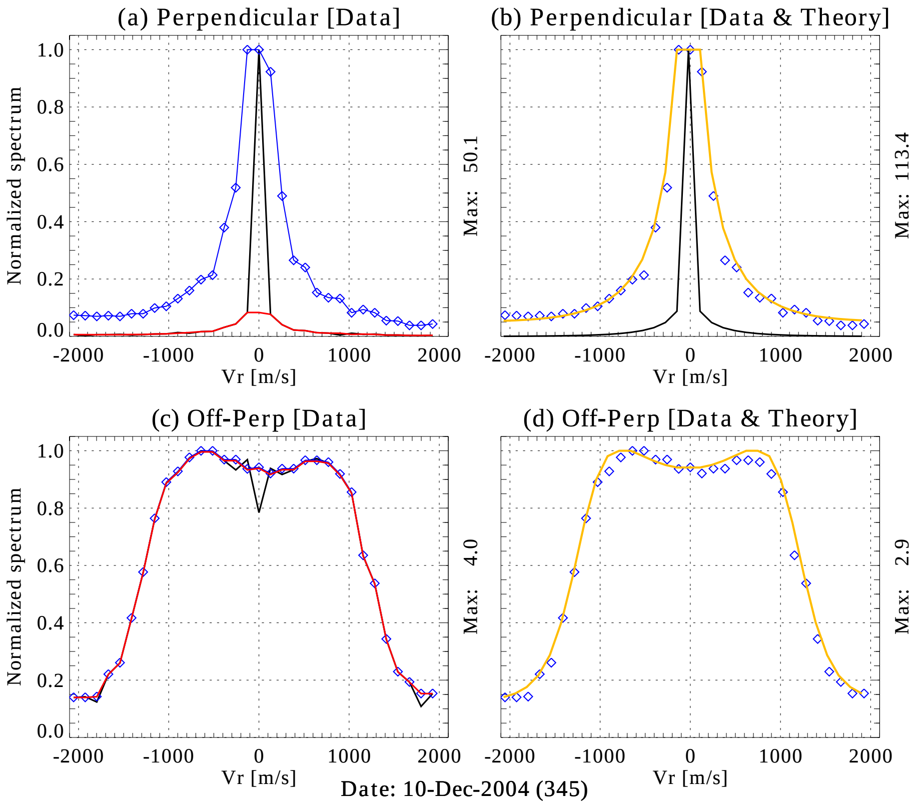

Fig. 6. Normalized 150-km spectra from **(a)** Perpendicular, and **(c)** Off-perpendicular data around 168 km after 3-min averaging. The time corresponds to the spectra shown in Fig. 3. A normalized spectrum after 3-point median filter is shown in red, while the normalized to its peak filtered series is shown in blue diamonds. In the second column we compare the normalized smooth spectra with a theoretical ISR spectrum in orange (see text for details).

angle possible with the Jicamarca main array), results not shown here.

So why the inconsistency with previous results? It should be realized that previous measurements were performed with beams perpendicular to B and only the low-frequency components were observed. As in the case of ISR signals due to gyrating electron control (magnetic field effects), the spectra gets narrower as the radar pointing gets closer to perpendicular, allowing the concentration of all the ionospheric signal in the low frequency bins. Given the strong dependence on pointing angle (Woodman, 2004; Milla and Kudeki, 2006), the low frequency information is indeed very aspect sensitive, so aspect sensitive that Woodman (1971) used interferometry on ISR perpendicular data to measure the inclination of the magnetic field. Therefore the results reported before are true values but only for the 150-km echoes coming from perpendicular. From our observations, except for the third layer, 150-km echoes are not as aspect sensitive as previously believed when all frequency components are considered.

In the case of echoes from the third layer, since they were not observed with off-perpendicular beams, these echoes are indeed very aspect sensitive and they could be as aspect sensitive as observed using interferometry. Then, why are the echoes of the third layer different than echoes from the other layers? First, we discuss the wide spectra results.

In Fig. 6 we show 3-min averaged spectra obtained from perpendicular and off-perpendicular signals. The spectra corresponds to cuts obtained from Fig. 3 around 168 km. The first column shows (a) the perpendicular, and (c) the off-perpendicular averaged spectra. The normalized-to-the-peak data are shown in black, while the 3-point median filtered data are shown in red. In blue we present the filtered signal normalized to its peak. This is particularly useful for the perpendicular data, so we can focus on the signal coming around perpendicular without the enhanced low frequency component. In the second column we compare the normalized filtered data (blue diamonds) with a theoretical ISR spectra (in orange). In all cases we are showing the normalization values to the right of each figure.

For the theoretical ISR spectra we have used the procedure described by Kudeki and Milla (2006), weighting the spectral contributions in accordance with the beam gain distribution. To get the excellent agreement for both the off-perpendicular and close to perpendicular data, we have used the following values: T_e=1200°K, T_e/T_i=2.0, 50% moleculars, 50% [O^+], and N_e=5×10^{11} m^{-3}. The agreement is excellent, except for the small asymmetry between humps. Routine ISR fits during standard off-perpendicular ISR experiments at Jicamarca show excellent agreement with the daytime measurements at these altitude (D. Hysell, personal communication, 2008). Moreover, in Fig. 5d, the off-perpendicular spectral width increases with increasing altitude consistent with the electron temperature dependence for these altitudes and latitude regions. We can naively try to use 150-km off-perpendicular spectra to diagnose this ionospheric region using the ISR technique, but without knowing the mechanism behind these echoes, the obtained parameters could be erroneous as reported at high latitudes when a wrong theory is fitted to the observations (e.g. Bahcivan et al., 2006; Saito et al., 2000).

The spectra from the off-perpendicular echoes resemble the ISR spectra expected at these altitudes, they are very wide and show almost symmetric humps, but they are enhanced, enhanced ion-line spectra. Besides the enhancement, these echoes present layering and power modulation in time that are not expected from thermal fluctuations. Are these echoes generated by plasma instabilities? We are ruling out this alternative for the enhanced ion-line spectra, since any approach to instability should be accompanied by a narrowing of the spectrum as the poles of the dispersion equation approach and even crosses the imaginary axes of the complex frequency plane.

At this point, we are inclined to explore mechanisms for allowing the enhancement of the ion-line spectra either via an amplification of the waves and/or by reducing the electron damping. Moreover such mechanisms have to be related to photoionization and photoelectron production. From previous and recent results there are three strong evidences related to the dependence of 150-km echoes on photoionization: (1) the necklace shape of the echoes as function of the time of the day, indicating a solar zenith angle dependence consistent with the photoelectron production dependence on solar zenith angle (Schunk and Nagy, 2000); (2) during solar maximum conditions echoes occur at lower altitudes (2–4 km) than during solar minimum conditions (following the work of Chau and Kudeki, 2006a); and (3) during the strong X17 solar flare event of 7 September 2005, 150-km echoes were observed to go down in altitude ∼10 km (Reyes et al., 2006).

But how photoelectrons can enhance the ion-line spectra? We do not have convincing arguments at the moment but have two working hypothesis to pursue in the future: (1) direct enhancement, or (2) an indirect enhancement. For the former, we plan to explore the possible contribution of photoelectrons to enhance the levels of the waves above the normal thermal equilibrium value, rather than bringing the plasma unstable (J. P. St. Maurice, personal communication, 2008). For the latter, it has been recognized that suprathermal electrons, such as photoelectrons, produced during the ionization of neutral species by solar extreme ultra violet (EUV) radiation can enhance ambipolar electric fields (Tam et al., 1995; Su et al., 1998). These ambipolar electric fields combined with fields from the E region (that are mapped via magnetic field lines) could generate significant parallel electric fields that in turn modify the velocity distribution of electrons at the altitudes of interest.

At high latitudes it has been shown that non-Maxwellian velocity distribution of electrons can increase the power of the ion-line spectra by 2–4 dB using the same parameters use for an assumed Maxwellian distribution (Saito et al., 2000; Bahcivan et al., 2006). However, it is very unlikely that these mechanisms will enhance the IS signal to the levels we are reporting.

Another possibility to enhance the ion-line spectra would be via the generation of Langmuir waves via photolectrons. Lee (1981) predicted that the ion-line spectra at low frequencies (50 MHz) would be enhanced strongly by the nonlinear interaction of intense unstable Langmuir waves. In fact, Woodman (2004)'s approach to the IS problem shows that the IS spectrum corresponds to the life time of an initial value problem. In the case of IS, the amplitude corresponds to the thermal level, but its behavior is the same as that of any wave amplitude set by any other means.

Coming back to the question, why are the echoes of the third layer different? Contrary to the 150-echoes showing enhanced ion-line spectra, the echoes of the third layer appear to be produced by plasma instabilities, they only show narrow spectra and are very strong. Moreover, these echoes are most probably similar to the majority of echoes observed with low power systems at other latitudes, where mainly one layer is observed (e.g. Tsunoda and Ecklund, 2008; de Paula and Hysell, 2004; Patra and Rao, 2006; Patra et al., 2008). The other layers are usually not observed due to lower sensitivity of the systems used. Multiple layers have been observed at Pohnpei but they do appear weaker (Tsunoda and Ecklund, 2000, 2007). The unique characteristic of this common layer of irregularities might be its composition. If somehow unusual strong concentration of metallic ions are present, it could provide the longer life time (longer than those expected from molecular ions) needed for an interchange instability (e.g. Kudeki and Fawcett, 1993; Tsunoda and Ecklund, 2008).

Our observations indicate that both type of 150-km echoes are being modulated by the same processes. Given the periodicities in power, Kudeki and Fawcett (1993) suggested that gravity waves might cause those modulations. Whatever is the mechanism that caused the enhanced echoes, gravity waves or another process, modulate the amplification factor and/or electron damping values.

We are aware that a careful quantitative analysis is required and we plan to do that in future efforts. Moreover, more observations are needed to determine the seasonal dependence and characteristics of the two different types of echoes.

5 Conclusions

The main conclusion of our work is that, 150-km echoes are composed of two different type of echoes: (1) those presenting similar spectra shapes similar to the expected IS spectra at those altitudes, but with 1 to 2 orders of magnitude enhancement (enhanced ion-line spectra), and (2) those presenting very narrow spectra shapes and observed only with beams pointing perpendicular to **B**. The latter might be caused by plasma instabilities. From the two datasets presented, the majority of the echoes are enhanced. Both types of echoes present similar temporal and altitudinal characteristics (e.g. power modulations, layering organization), although independent of their generation mechanism, they are both modulated by the same processes.

A derived conclusion is that most 150-km echoes are not as aspect sensitive as originally thought. Only when low frequency components are observed, 150-km echoes are very aspect sensitive with values less than 0.1° as reported by previous interferometric work.

Acknowledgements. We wish to thank D. Hysell and J. P. St. Maurice for their insightful suggestions during different stages of this work. The Jicamarca Radio Observatory is a facility of the Instituto Geofísico del Perú operated with support from the NSF Cooperative Agreement ATM-0432565 through Cornell University.

Topical Editor K. Kauristie thanks W. Swartz and R. Tsunoda for their help in evaluating this paper.

References

Anderson, D. N., Anghel, A., Chau, J. L., and Veliz, O.: Daytime, Vertical ExB Drift Velocities Inferred from Ground-Based Magnetometer Observations at Low Latitudes, Space Weather, 2, S11001, doi:10.1029/2004SW000095, 2004.

Bahcivan, H., Cosgrove, R. B., and Tsunoda, R. T.: Parallel electron streaming in the high-latitude *E* region and its effect on the incoherent scatter spectrum, J. Geophys. Res., 111, A07306, doi:10.1029/2005JA011595, 2006.

Balsley, B. B.: Evidence of a Stratified Echoing Region at 150 Kilometers in the Vecinity of Magnetic Equator During Daylight Hours, J. Geophys. Res., 69, 1925–1930, 1964.

Blanc, E., Mercandalli, B., and Houngninou, E.: Kilometric Irregularities in the *E* and *F* Regions of the Daytime Equatorial Ionosphere Observed by a High Resolution HF Radar, Geophys. Res. Lett., 23, 645–648, 1996.

Chau, J. L.: Unexpected Spectral Characteristics of VHF Radar Signals from 150-Km Region over Jicamarca, Geophys. Res. Lett., 31, L23803, doi:10.1029/2004GL021620, 2004.

Chau, J. L. and Kudeki, E.: Statistics of 150-km echoes over Jicamarca based on low-power VHF observations, Ann. Geophys., 24, 1305–1310, 2006a.

Chau, J. L. and Kudeki, E.: First E- and D-region incoherent scatter spectra observed over Jicamarca, Ann. Geophys., 24, 1295–1303, 2006b.

Chau, J. L. and Woodman, R. F.: Daytime Vertical and Zonal Velocities from 150-Km Echoes: Their Relevance to *F*-Region Dynamics, Geophys. Res. Lett., 31, L17801, doi:10.1029/2004GL020800, 2004.

Chau, J. L. and Woodman, R. F.: *D*- and *E*-Region Incoherent Scatter Radar Density Measurements over Jicamarca, J. Geophys. Res., 110, A12314, doi:10.1029/2005JA011438, 2005.

Choudhary, R. K., St. Maurice, J. P., and Mahajan, K. K.: Observations of coherent echoes with narrow spectra near 150 km altitude during daytime way from the dip equator, Geophys. Res. Lett., 31, L19801, doi:10.1029/2004GL020299., 2004.

de Paula, E. R. and Hysell, D. L.: The Sao Luis 30 MHz Coherent Scatter Ionospheric Radar: System Description and Initial Results, Radio Sci., 39, RS1014, doi:10.1029/2003RS002914, 2004.

Farley, D. T.: Faraday Rotation Measurements Using Incoherent Scatter, Radio Sci., 4, 143–152, 1969.

Fawcett, C.: An Investigation of Equatorial 150-Km Irregularities, PhD thesis, Univ. of Illinois at Urbana-Champaign, 1999.

Kudeki, E. and Fawcett, C. D.: High resolution observations of 150 Km echoes at Jicamarca, Geophys. Res. Lett., 20, 1987–1990, 1993.

Kudeki, E. and Milla, M. A.: Incoherent scatter spectrum theory for modes propagating perpendicular to the geomagnetic field, J. Geophys. Res., 111, A06306, doi:10.1029/2005JA011 546, 2006.

Kudeki, E., Fawcett, C. D., Ecklund, W. L., Johnston, P. E., and Franke, S. J.: Equatorial 150-Km Irregularities Observed at Pohnpei, Geophys. Res. Lett., 25, 4079–4082, 1998.

Lee, M. C.: Ion line enhancement in ionospheric heating experiments, J. Phys. D: Appl. Phys., 14, 851–860, 1981.

Lu, F., Farley, D. T., and Swartz, W. E.: Spread in aspect angles of equatorial *E* region irregularities, J. Geophys. Res., 113, A11309, doi:10.1029/2008JA013018, 2008.

Milla, M. and Kudeki, E.: F-region electron density and T_e/T_i measurements using incoherent scatter power data collected at ALTAIR, Ann. Geophys., 24, 1333–1342, 2006, http://www.ann-geophys.net/24/1333/2006/.

Patra, A. K. and Rao, N. V.: Radar observations of daytime 150-km echoes from outside the equatorial electrojet belt over Gadanki, Geophys. Res. Lett., 33, L03104, doi:10.1029/2005GL024564, 2006.

Patra, A. K. and Rao, N. V.: Further investigations of 150-km echoing riddle using simultaneous observations of 150-km and *E* region echoes from off-electrojet location Gadanki, J. Geophys. Res., 112, A09301, doi:10.1029/2006JA012204, 2007.

Patra, A. K., Yokoyama, T., Otsuka, Y., and Yamamoto, M.: Daytime 150-km echoes observed with the Equatorial Atmosphere radar in Indonesia: First results, Geophys. Res. Lett., 35, L06101, doi:10.1029/2007GL033130, 2008.

Prakash, S., Gupta, S. P., and Subbaraya, B. H.: Irregularities in the equatorial *E* region over Thumba, Radio Sci., 4, 791–796, 1969.

Reyes, P., Akgiray, A., Kudeki, E., Lehmacher, G., Woodman, R., and Chau, J.: Study of a X17 Solar Flare Effects Observed over Jicamarca on Sept. 07 2005, Paper presented at the CEDAR Workshop, Santa Fe, NM, USA, 2006.

Røyrvik, O.: Drift and aspect sensivity of scattering irregularities in the upper equatorial *E* region, J. Geophys. Res., 87, 8338–8342, 1982.

Røyrvik, O. and Miller, K. L.: Nonthermal Scattering of Radio Waves Near 150 Km Above Jicamarca, Peru, J. Geophys. Res., 86, 180–188, 1981.

Saito, S., Forme, F. R. E., Buchert, S. C., Nozawa, S., and Fujii, R.: Effects of a kappa distribution function of electrons on incoherent scatter spectra, Ann. Geophys., 18, 1216–1223, 2000, http://www.ann-geophys.net/18/1216/2000/.

Schunk, R. W. and Nagy, A. F.: Ionospheres – Physics, Plasma Physics, and Chemistry, Cambridge Univ. Press, 2000.

Su, Y. J., Horwitz, J. L., Wilson, G. R., Richards, P. G., Brown, D. G., and Ho, C. W.: Self-consistent simulation of the photoelectron-driven polar wind from 120 km to 9 R_E altitude, J. Geophys. Res., 103, 2279–2296, 1998.

Sulzer, M. P. and Gonzalez, S. A.: The Effect of Electron Coulomb Collisions on the Incoherent Scatter Spectrum in the F Region at Jicamarca, J. Geophys. Res., 104, 22535–22552, 1999.

Tam, S. W. Y., Yasseen, F., Chang, T., and Ganguli, S. B.: Self-consistent kinetic photoelectron effects on the polar wind, Geophys. Res. Lett., 22, 2107–2110, 1995.

Tsunoda, R. T. and Ecklund, W. L.: On the Nature of 150-Km Radar Echoes over the Magnetic Equator, Geophys. Res. Lett., 27, 657–660, 2000.

Tsunoda, R. T. and Ecklund, W. L.: On a Summer Maximum in the Occurrence Frequency of 150 Km (F_1) Radar Echoes over Pohnpei, Geophys. Res. Lett., 31, L06810, doi:10.1029/2003GL018704, 2004.

Tsunoda, R. T. and Ecklund, W. L.: On the visibility and zenithal confinement of 150 km (F_1) radar echoes, Geophys. Res. Lett., 34, L21102, doi:10.1029/2007GL031276, 2007.

Tsunoda, R. T. and Ecklund, W. L.: On the sheet like nature of 150-km (F_1) radar echoes, Geophys. Res. Lett., 35, L05102, doi:10.1029/2007GL032152, 2008.

Woodman, R. F.: Inclination of the geomagnetic field measured by an incoherent scatter technique, J. Geophys. Res., 76, 178–184, 1971.

Woodman, R. F.: On a Proper Electron Collision Frequency for a Fokker-Plank Collision Model with Jicamarca Applications, J. Atmos. Sol. Terr. Phys., 66, 1521–1541, 2004.

Woodman, R. F. and Chau, J. L.: New observations of the 150-km echoes observed at the Jicamarca Radio Observatory, paper presented at the Eleventh Int. Symposium on Equatorial Aeronomy, Taipei, Taiwan, 2005.

Woodman, R. F. and Villanueva, F.: Comparison of Electric Fields Measured at F Region Heights with 150 Km Irregularity Drift Measurements, paper presented at the Ninth Int. Symposium on Equatorial Aeronomy, Bali, Indonesia, 1995.